



Aluminium (III) dialkyl 2,6-bisimino-4R-dihydropyridinates(-1): Selective Synthesis, Structure and Controlled Dimerization.

Journal:	<i>Dalton Transactions</i>
Manuscript ID	DT-ART-02-2019-000847.R1
Article Type:	Paper
Date Submitted by the Author:	08-Apr-2019
Complete List of Authors:	Gallardo-Villagrán, Manuel ; University of Seville, Química Inorgánica Vidal, Fernando; Rutgers University Newark, Department of Chemistry Palma, Pilar; Centro de Investigaciones Científicas Isla de la Cartuja, Instituto de investigaciones químicas Alvarez González, Eleuterio; Centro de Investigaciones Científicas Isla de la Cartuja, Instituto de investigaciones Químicas Chen, Eugene; Colorado State University, Chemistry Campora, Juan; Centro de Investigaciones Científicas Isla de la Cartuja, Instituto de Investigaciones Químicas Rodríguez Delgado, Antonio; University of Seville, Química Inorgánica; Centro de Investigaciones Científicas Isla de la Cartuja, Instituto de Investigaciones Químicas

Title: Aluminium (III) dialkyl 2,6-bis(imino)-4R-dihydropyridinates(-1): Selective Synthesis, Structure and Controlled Dimerization.

Authors: Manuel Gallardo-Villagrán,^a Fernando Vidal,^b Pilar Palma,^a Eleuterio Álvarez,^a Eugene Y.-X. Chen,^c Juan Cámpora,^a and Antonio Rodríguez-Delgado^{*a}

^a Instituto de Investigaciones Químicas, CSIC-Universidad de Sevilla. c/ Américo Vespucio, 49, 41092, Sevilla, Spain.

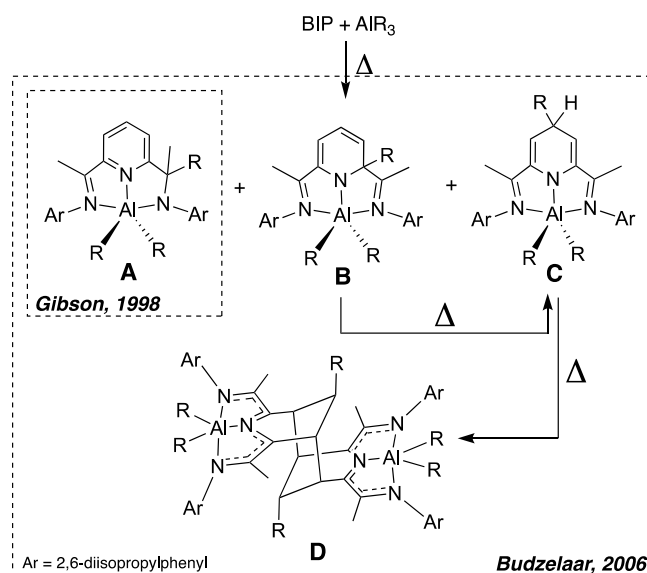
^b Department of Chemistry, Rutgers University, 73 Warren Street, Newark, New Jersey 07102

^c Department of Chemistry, Colorado State University, Fort Collins, Colorado 80523-1972

Introduction

More than two decades have passed since the earliest reports on the synthesis of organometallic complexes supported by 2,6-bis(imino)pyridine ligands (BIP).¹ Since then, the research on the interaction of such ligands with aluminium (III) alkyls (R_3Al) has attracted the interest of different research groups.²⁻⁵ The first reports were reported by Gibson, shortly after of Brookhart's and his landmark publications on the discovery of BIP iron and cobalt complexes $[MCl_2(BIP)]$ with methylaluminoxane (MAO) highly active catalysts for ethylene polymerization.⁶ The extension towards the synthesis of the organoaluminium derivatives was envisioned as a straightforward access to the corresponding transition metal-free alkyl BIP complexes, systems of notorious potential in such catalytic reactions.² Gibson's initial results, followed by other analogous by Grassi,³ showed that a relatively straightforward reaction ensues when iPr BIP is reacted with an excess of $AlMe_3$ under rather forced conditions (refluxing toluene). This leads to dialkylaluminum species supported by imino-amido tridentate ligand arising from single methylation of one of imine groups of the iPr BIP ligand. These systems exhibit some olefin polymerization activity when activated with powerful Lewis acids. A few years later, Budzelaar discovered that the reaction of R_3Al with BIP was deceptively simple.⁴ He observed that treatment of BIP ligands with different aluminum trialkyls under milder reaction conditions, more akin to those applied for polymerization catalysis, invariably led to mixtures of several organometallic species arising from unselective alkyl transfer from the metal to different positions of the BIP ligand (Scheme 1).^{4b} Whilst species of the type **B** were invariably the main products of the reaction, the imine-amide species (**A**) identified by Gibson and Grassi were also formed, along with species of type **C**, the products arising from alkyl migration to the remote position 4 in the pyridine ring. Albeit heating the reaction mixtures apparently causes the isomerization of product **B** into **C**, the transformation was never complete, and in addition a fourth binuclear species **D** emerged. These complicated mixtures could not be separated, and the different species were identified on the basis of comparative spectroscopic and computational work, together with the resolution of the structure of few crystals that grew, among those a couple

of examples of the dimers **D**, whose NMR spectrum could never be adequately recorded. The resolution of the structure of such dimers allowed to establish that the pathway from the initial BIP ligand to these binuclear species **D** crossed through the dihydropyridinate **C**, which is its immediate precursor. Although a similar process could explain the formation of an analogous binuclear Cr complex as a result of the reaction of $[(iPr)BIP]CrCl_3$ with $BnMgCl$, the mechanism had remained speculative as the corresponding chromium dihydropyridinate analogue of **C** had not been identified.⁷

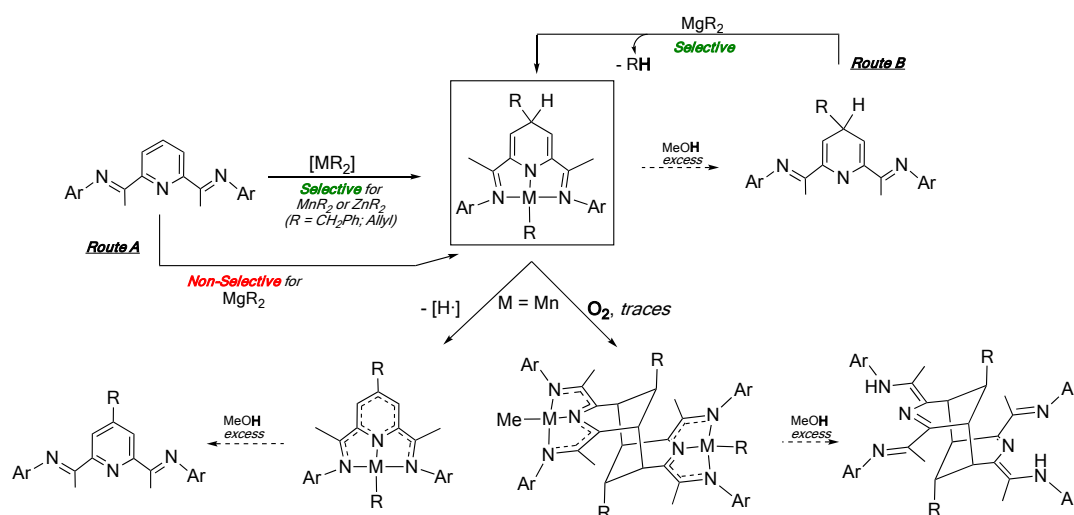


Scheme 1.

Even though the complex chemistry disclosed by Budzelaar has clarified many details of the peculiar reactivity of ^RBIP ligands in combination with aluminum alkyls, it may seem of little practical synthetic value. However, different groups including ours have investigated the organometallic of ^RBIP ligands, and much progress has been achieved in recent years.^{1c} For example, one of the best-known properties of ^RBIP ligands is their non-innocent character, that plays a critical role in enabling many of the most recent applications of these ligands in catalysis. Whilst this attribute, based on the ability of such ligands to participate in redox transformations, has been well-documented for transition metal complexes,⁸ it gains even more significance for redox inactive main group metal BIP ions.⁹ Non-innocent alkylaluminum of the type $[AlR_2(iPr)BIP]$, that contain an Al(III) fragment and a reduced $iPr)BIP^{\cdot-}$ radical-anion ligand were isolated by Gambarotta¹⁰ and by us,¹¹ and a number of derivatives of other non-redox main-group metals have been reported by others.⁸

In particular, we became interested in the aluminum compounds of type **C**, for several reasons. First, these systems are akin to others that we and others have selectively generated with transition metals such as manganese,¹² iron¹³ or later with post-transition elements like zinc,¹⁴ upon straightforward reactions of the corresponding metal dialkyls (MR_2)^{12,14} or monoalkyls $(py_2(FeCH_2CMe_3)Cl)$ ¹³ with BIP ligands, (Scheme 2, *Route A, for Mn and Zn*). On the other hand, when this direct method did not lead to the expected selective result, like in the case of main group elements such as magnesium,^{14,15} we tackled the

problem through an alternative strategy. (Scheme 2, *Route B*). This method relied in the demetallation of their Mn or Zn dihydropyridinate complexes with methanol, followed by the isolation the free bases and then reacting them with suitable magnesium dialkyls (MgR_2 ; R = Bn, Bu).¹⁶ Such reactions were fast and clean, and proved very convenient from the synthetic point of view as they cleanly afforded the expected 4-R-1,4-dihydropyridinate(-1) magnesium (II) monoalkyls that could not be selectively obtained when the *Route A* in Scheme 2 was applied. Furthermore, as we showed few years ago,¹⁷ manganese dihydropyridinates, although highly sensitive compounds and prone to undergo spontaneous aromatization (Scheme 2, bottom left), can be induced to experience a similar dimerization than that of the aluminum and chromium complexes (Scheme 2, bottom right). Using the above-mentioned ligand transfer strategy, we demetallated the resulting manganese dimers and the tricyclic bases were then transferred to different metal complexes (Zn, Pd). Due to the technical difficulties on controlling the oxygen-induced dimerization reaction, the ligand-transfer methodology was restricted to a single BIP ligand.



Scheme 2.

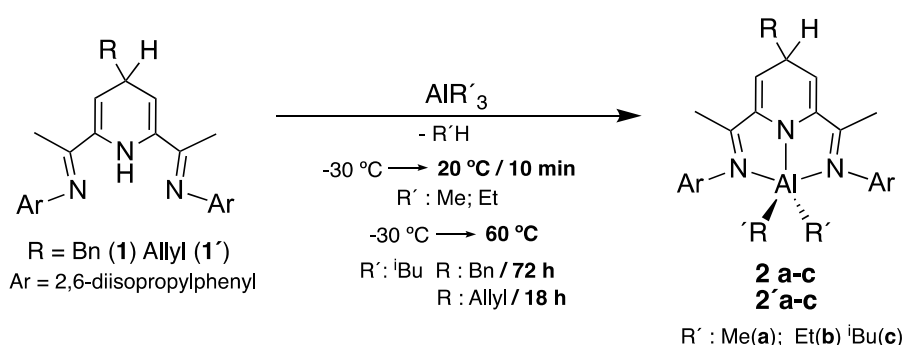
In this contribution, we report the application of *Route B* in Scheme 2 for the selective synthesis and full characterization of aluminum complexes of type **C**, followed by their treatment to obtain complexes of the type **D**, both akin (but not identical) to those previously identified by Budzelaar as part of more or less complex mixtures of products. We verified that the aluminum dihydropyridinates though moderately stable, undergo a well-behaved, clean thermal dimerization. This transformation, followed by a mild demetallation protocol, provides a clean pathway to the corresponding tricyclic bases, allowing systematic investigation of these promising molecules as a novel type of ditopic pincer ligands.

Results and discussion

Reaction of dihydropyridines 1 and 1' with aluminium alkyls.- We initiated our investigation revisiting the syntheses of dihydropyridines 4-R-ⁱPrH₂BIP with R = benzyl (**1**) or allyl (**1'**). We

had reported that these metal-free compounds can be accessed from BIPs using organomanganous chemistry¹² and in addition, we optimized a procedure for the syntheses for R = benzyl, but the allyl derivative was usually obtained with variable amounts of the aromatized 4-R-ⁱPrBIP.¹⁴ In the same contribution, we also showed that the ZnR₂-based route resulted promising, as the Zn dihydropyridinate systems are not prone to undergo spontaneous dehydrogenation. Yet, the released allyl dihydropyridine was readily oxidized during the workup. We now describe some practical improvements related to this protocol that had allowed the syntheses of both 4-R-ⁱPrH₂BIP ligands (**1** and **1'**).

Next, we addressed the reaction of **1** and **1'** with aluminium trialkyls derivatives AIR'₃ (R' = Me, Et, *i*-Bu, Scheme 3). Upon mixing cold (-30 °C) solutions in toluene-*d*₈ containing equimolar amounts of both components, intense burgundy (R'= Me, Et) colorations or indigo (R' = *i*Bu) develop. ¹H NMR monitoring showed that for R = Me or Et the reaction is complete after a short time at room temperature. The spectra are consistent with clean formation of the corresponding dihydropyridinate complexes with concomitant elimination of alkane. For example, the ¹H NMR spectrum of **2a** and **2'a** exhibit two close singlets integrating for 3H each in the highest field region of their spectra (ca. -0.69 to -0.71 ppm) for the aluminium-bound methyl groups, which loss their chemical equivalence under the influence of the 4-R-dihydropyridinate ligand. In return, the latter give rise to signal patterns very similar to those of the free ligands, except for the absent NH resonance. Likewise, the diethyl derivatives **2b** and **2'b** exhibit similar ¹H-NMR features, excluding the quartets and triplets for two non-equivalent ethyl groups attached to aluminium. The spectra of these dihydropyridinate complexes are strongly reminiscent of those of the alkyl Zn and -Mg congeners reported by us.^{14,15} An even more pertinent comparison can be established with the partial spectral data reported by Budzelaar for closely related dialkylaluminium dihydropyridinates, that although is based mostly on the analysis of spectra of complex reaction mixtures and DFT calculations,⁴ confirms our assignments.



Scheme 3.

NMR samples **2a**, **b** and **2'a**, **b** in toluene or benzene are notoriously stable, as their spectra show no visible changes over several days at ambient temperature. This encouraged us to pursue their isolation. These complexes were readily made in preparative scale and crystallized from hexane, from which they were isolated as dark burgundy crystalline solids

and fully characterized by the usual ensemble of ^1H and ^{13}C NMR, elemental analysis and X-ray diffraction for **2'a**. Worth noting is the relatively low boiling point of both Me_3Al or Et_3Al used as complexes' precursors which makes the dihydropyridine ligand deprotonation very convenient from the technical point of view, since these reactions do not require an accurate stoichiometric control. We demonstrated that a small excess of trialkylaluminium in the reactor does not affect either the rate, nor the product yields, while it guarantees the total consumption of the ligand. Thus, the extra organoaluminium species remaining upon the reaction completion, adventitiously or deliberately added, was conveniently removed at reduced pressure.

Figure 1 shows the crystal structure of **2'a**. The N_3 tridentate ligand features similar bond distances to those found in the previously reported $\text{Zn}(\text{II})$ and $\text{Mg}(\text{II})$ dihydropyridinates. As it is frequently observed in complexes with BIP and BIP-based ligands, the bonds connecting the metal center with the imine nitrogen atoms N1 and N3 are slightly different (2.235(17) and 2.208(17) Å, respectively), and appreciably longer than the Al-N2, which involves the heterocyclic N2 atom. The geometry of the pentacoordinated Al center can be regarded as distorted square pyramidal ($\tau_5 = 0.43$) with the methyl ligands placed in the basis and in the apex, respectively. This is in close analogy with Gambarotta's dimethylaluminum complex $[(^i\text{PrBIP})^{-1}(\text{Al}^{\text{III}})\text{Me}_2]$, which contains a reduced $^i\text{PrBIP}$ ligand. In contrast, the diethylaluminium analogue $[(^i\text{PrBIP})^{-1}(\text{Al}^{\text{III}})\text{Et}_2]$, reported by us, presents a nearly perfect square pyramid geometry with $\tau_5 = 0.04$.

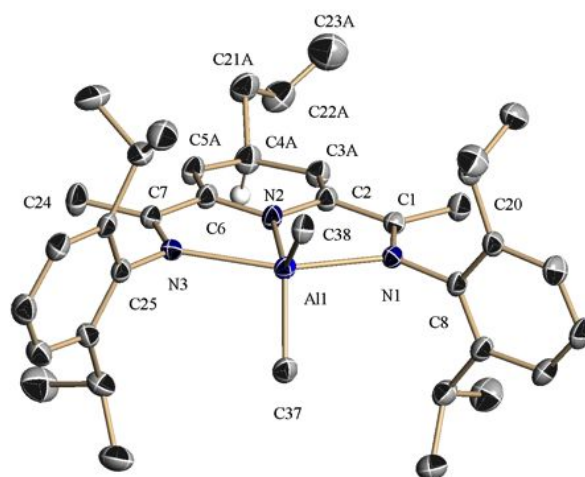


Figure 1. ORTEP representation of the structure of compound **2'a**. Selected bond lengths (Å) and angles ($^\circ$): Al(1)-C(37), 1.974(2); Al(1)-C(38), 1.975(2); Al(1)-N(1), 2.235(17); Al(1)-N(2), 1.887(17); Al(1)-N(3), 2.208(17); N(2)-C(2), 1.388(3); C(1)-C(2), 1.468(3); C(2)-C(3A), 1.362(5); C(3A)-C(4A), 1.501(5); N(2)-Al(1)-C(38), 126.76(9); N(3)-Al(1)-N(1), 152.63(6); N(2)-Al(1)-C(37), 125.32(9); C(37)-Al(1)-C(38), 107.91(10); N(2)-Al(1)-N(1), 75.92(7); N(2)-Al(1)-N(3), 76.71(7); N(1)-Al(1)-C(38), 98.22(8); N(3)-Al(1)-C(38), 97.67(8).

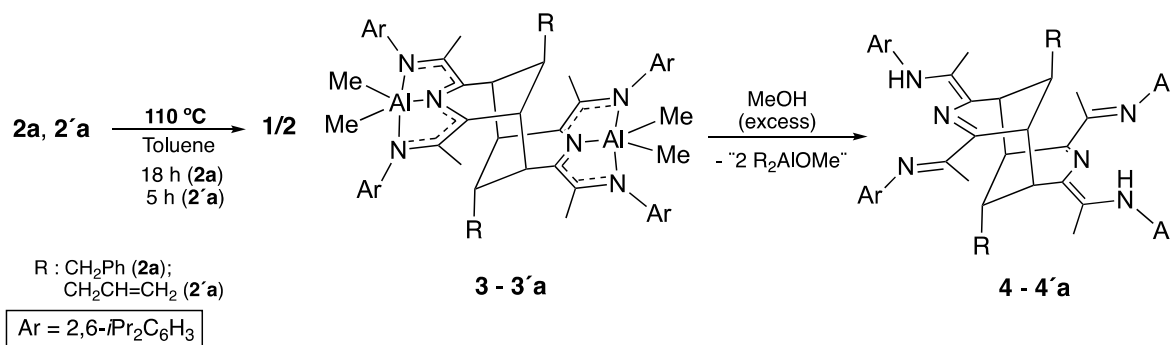
Contrarily to the fast reactions of the dihydropyridines **1** and **1'** with AlMe_3 and AlEt_3 , ^1H NMR monitorization of the corresponding reactions with $\text{Al}(i\text{-Bu})_3$ revealed no signs of products after warming the mixtures to room temperature, in spite of the intense blue indigo colour developed upon reagents mixing at $-30\text{ }^\circ\text{C}$. After 2h at $23\text{ }^\circ\text{C}$, the indigo colour of the reaction solutions persisted, and the samples still reveal mostly unaltered signals for the reagents ($\text{Al}(i\text{-Bu})_3$ and **1** or **1'**), together with small sets of resonances, attributable to the corresponding products **2c** or **2'c**. Full conversions were only attained after prolonged heating at $60\text{ }^\circ\text{C}$. At this temperature, the colour of the solutions gradually evolves to burgundy hues, similar to that observed in the reactions with AlMe_3 or AlEt_3 . The reaction was appreciably faster for the allyl ligand **1'**, (**2'c** in 18 h) than for the benzyl congener, which required 72 h. As a consequence, we proceeded to isolated **2'c**, but did not pursue the preparation of pure samples of **2c**, which was characterized in solution. Comparison of the spectroscopic features of **2c** with those of **2'c** and the remaining dihydropyridinates **2-2'** allowed its unambiguous identification.

Thermal behaviour of dihydropyridinate complexes: dimerization vs. aromatization.- As mentioned in the Introduction, Budzelaar has shown that heating the mixtures resulting from the reaction of $i\text{PrBIP}$ with aluminium alkyls (in particular, AlClEt_2 ^{4a} and $\text{AlH}i\text{Bu}_2$ ^{4b}) allows obtaining small amounts of tricyclic dimers, arising from monomeric precursors of type **C** analogous to complexes **2** or **2'** (Scheme 3). Such dimers were characterized by X-ray diffraction but, they seemed to be too insoluble, or perhaps contaminated with paramagnetic impurities that prevented their characterization by NMR. As mentioned, similar dimeric compounds have been isolated in low yields after the reaction of paramagnetic Cr(III) with benzylmagnesium chloride.⁷ Our group has shown that dimerization of alkylmanganese(II) dihydropyridinates only does take place if it is triggered by traces amounts of oxygen as shown in Scheme 2. Otherwise, the monomeric precursors experience spontaneous hydrogen loss yielding aromatized organomanganese(I) BIP species.^{12b} Due to the difficulty of monitoring the transformation by NMR, neither for the paramagnetic Cr or Mn systems, nor in Budzelaar's was possible to gather relevant data to ascertain the mechanism of the dimerization process, though the latter author has supported a bimolecular mechanism based on DFT calculations. This involved the consecutive formation of two C-C bonds required to assemble the tricyclic unit, *via* a single-bonded intermediate with diradical character. This mechanism does not require any activation of the monomers, but the complexity of the overall reaction with aluminium does not allow to rule out the participation of any of the species present in the reactions mixtures.

The selective synthesis of complex **2** or **2'** put us in the position to study whether these complexes are prone to undergo dimerization, or like their organomanganese(II) analogues, they require to interact with an external agent such the traces amount of oxygen to proceed. To clarify this point, we firstly examined the behaviour of pure (isolated) samples of

complexes **2a**, **b** and **2'a-c** dissolved in toluene- d_8 under heating in gas-tight NMR tubes, sealed with PTFE valves.

When samples complexes **2a** and **2'a** were heated in a thermostated oil bath, their burgundy colour gradually became a deeper hue. The $^1\text{H-NMR}$ spectra showed new sets of signals growing at the expense of the initial ones, consistent with the new dimeric species **3a** and **3'a**, respectively (Scheme 4). The transformation takes ca. three days to complete at 80 °C or 36h at 110 °C for the 4-benzyl derivative, but proceeds faster for the 4-allyl, being essentially finished in 3 h at 80 °C. For preparative purposes, these reactions were carried out in teflon-valved glass ampoules also in a thermostated oil bath, heating the toluene solutions of the monomeric precursors **2a** and **2'a** at 110 °C. A regular workup provided analytically pure samples of both compounds which were subject to full characterization. For example, Figure 2 shows a comparison of the $^1\text{H-NMR}$ spectra of **2a** and **3a**. As can be seen, the spectral features of the dimer appear clearly, confirming its identity. As the 3,5 vinyl-type carbons in **2a** become aliphatic bridgehead atoms in **3a**, the characteristic pattern of signals corresponding to the dihydropyridine moiety of **2a**, namely, a doublet at 2.80 ppm for the benzyl CH_2 , a multiplet at 4.00 ppm for the heterocyclic 4-CH and a doublet at 5.07 ppm for the neighbouring ring protons are replaced by a doublet, a multiplet and a singlet, respectively, in the spectrum of the **3a** dimer. The spectrum of **3'a** exhibits very similar signal pattern for the heterocyclic fragment, and essentially unperturbed signals for the pending allyl groups, confirming that the terminal double bond is a mere spectator during in dimerization reaction. As shown also in Scheme 4, treatment of **3a** or **3'a** with an excess of methanol leads to mixtures of the corresponding tricyclic bases **4** and **4'**. We previously applied the same method for the analysis of the paramagnetic, NMR silent complexes formed in the related Mn(II) system. In particular, the signals in the $^1\text{H-NMR}$ spectrum of compound **4'** are undistinguishable from those of a sample containing product obtained from the Mn route. As noted previously, the NMR spectra of these polyimino bases appear rather more complex than would be expected because they exist in solution as a mixture of organic tautomers. The ESI-MS analysis of the crude material for **4** showed the expected signal at m/z 1146.8 for the protonated molecular ion $[\text{M} + \text{H}]^+$. In addition to their analytic value, the demetallation reactions provide a new and more selective approach to the dimers **4** and **4'**, which could not be accessed selectively through the organomanganese route.



Scheme 4.

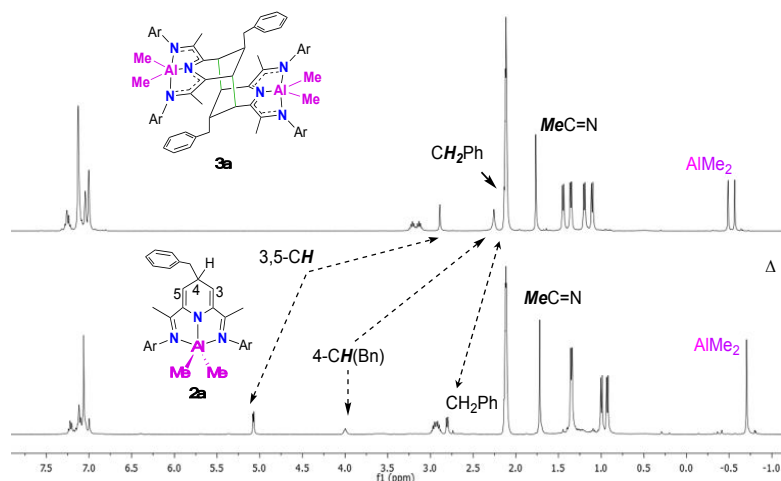


Figure 2. 1H NMR (toluene- d_8 , 25 $^\circ C$, 400 MHz) spectra showing the transformation of **2a** in **3a** (below, compound **2a**; top, same sample after heating at 80 $^\circ C$ for 72 h).

Suitable crystals for X-ray diffraction studies of both dimers were grown from cold dichloromethane (**3a**, Figure 3) or hexane solutions (**3'a**, Figure 4). These display a tricyclic ditopic ligand symmetrically bridging two $AlMe_2$ fragments, related by a molecular inversion centre. The pentacoordinated aluminium centres exhibit distorted square pyramidal geometries ($\tau_5 = 0.07$ and 0.05 for **3a** and **3'a**, respectively). Both dimers are similar to related Cr ,⁷ Al ⁴ and Pd ¹⁷ complexes previously reported in the literature. All of them share in common a central cyclohexane core in a chair conformation, arising from the fusion of the dihydropyridinate ring through carbons 3 and 5. In both structures, the 4-R substituents end up as equatorial substituents, presumably in order to minimize the unfavourable steric repulsion that would result otherwise. This implies a high level of stereocontrol in the dimerization reaction, as the approach of the monomeric precursors must proceed exclusively by the least hindered face of the heterocyclic dihydropyridine ring.

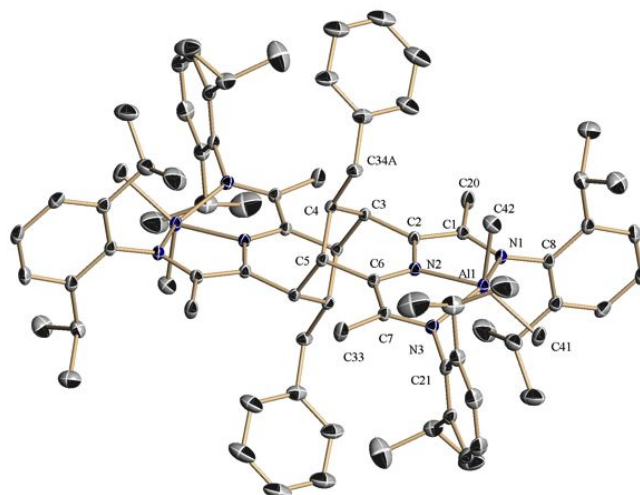


Figure 3. ORTEP representation of the structure of compound **3a** Selected bond lengths (Å) and angles (deg): Al-N(1): 2.106(13); Al-N(2): 2.010(13); Al-N(3): 2.120(13); Al-C(41): 1.976(17); Al-C(42): 1.988(13); N(1)-C(1): 1.315(19); N2-C(6): 1.338(19); N(2)-C(2): 1.341(19); N(3)-C(7): 1.310(19); C(1)-C(2): 1.427(2); C(1)-C(20): 1.503(2); C(2)-C(3): 1.511(2); C(3)-C(4): 1.543(2); C(3)-C(5): 1.566(2); C(4)-C(5): 1.543(2); C(5)-C(6): 1.510(2); C(6)-C(7): 1.436(2); C(7)-C(33): 1.504(2); N(2)-Al-N(1): 76.40(5); N(2)-Al-C(41): 143.85(7); N(2)-Al-C(42): 98.56(7); C(41)-Al-C(42): 117.59(9); N(2)-Al-N(3): 76.48(5); N(1)-Al-N(3): 148.01(5).

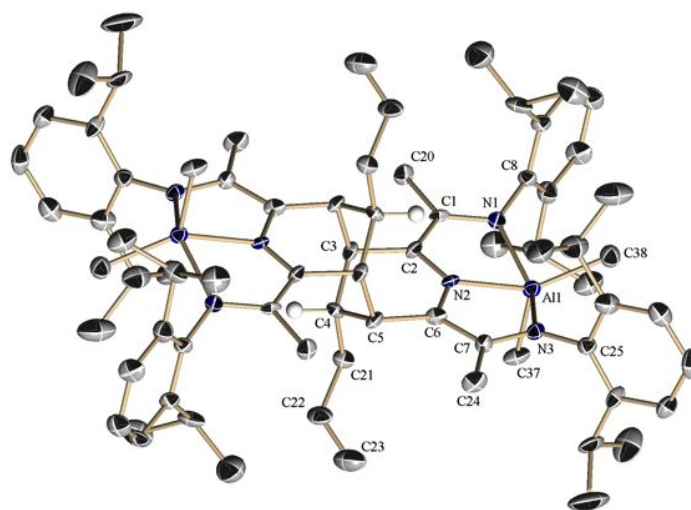
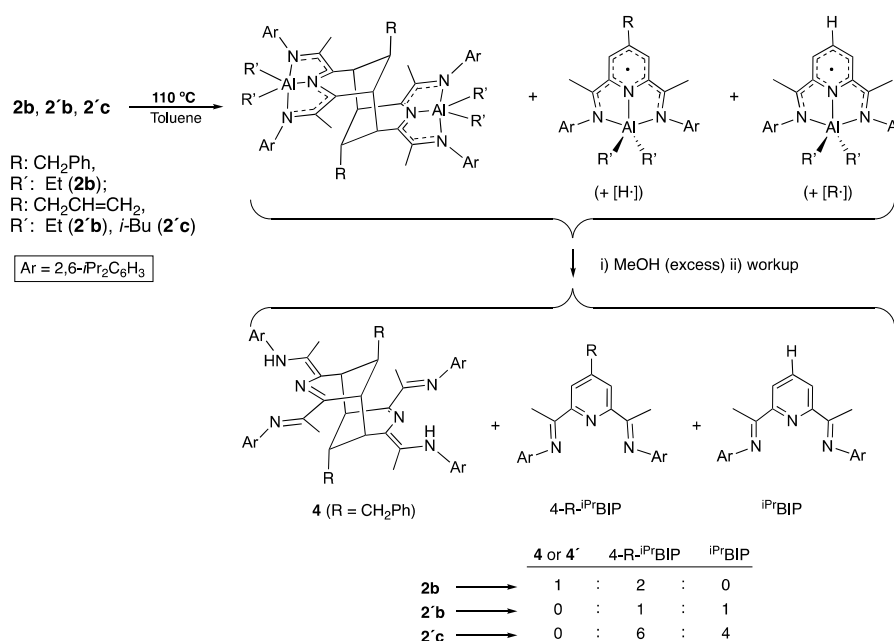


Figure 4. ORTEP representation of the structure of compound **3'a** Selected bond lengths (Å) and angles (deg): Al-N(1): 2.106(4); Al-N(2): 2.009(4); Al-N(3): 2.106(4); Al-C(38): 1.975(5); Al-C(37): 1.992(5); N(1)-C(1): 1.329(5); C(1)-C(20): 1.496(6); N2-C(6): 1.327(5); N(2)-C(2): 1.342(5); C(2)-C(3): 1.510(6); C(3)-C(5): 1.541(6); C(3)-C(4): 1.541(6); C(4)-C(5): 1.547(6); C(5)-C(6): 1.518(6); N(3)-C(7): 1.313(5); C(1)-C(2): 1.423(6); C(6)-C(7): 1.436(6); C(7)-C(24): 1.505(6); N(1)-Al-N(2): 76.65(14); N(2)-Al-N(3): 76.10(14); N(2)-Al-C(37): 96.45(18); N(2)-Al-C(38): 143.83(18); C(37)-Al-C(38): 119.7(2); N(1)-Al-N(3): 146.69(15).

The notorious rate differences observed for the dimerization of **2a** and **2'a** indicates that this process is highly sensitive to steric effects. Thus, it is not completely surprising that dimer formation becomes increasingly more difficult as the size of the metal fragment increases. As we studied the thermal behavior of diethylaluminum complexes **2b**, **2'b** or the isobutyl

derivative **2'c** at 110 °C in toluene-*d*₈, we found that different processes become significant (Scheme 5). In particular, when a sample of **2b** was heated at the mentioned temperature for three days, a slight colour change denoted that a similar transformation to that undergone by the methyl derivatives had taken place. The ¹H-NMR spectrum apparently confirmed this conclusion, as the signals of the starting material had been replaced by a new set of resonances attributable to the corresponding dimer, **3b**, on the basis of their analogy with those of the previously characterized products. However, despite the fact that such signals were the only ones in the final spectrum, their intensity appeared too weak in relation to those residual solvent peaks. Thus, we applied the standard methanol demetallation treatment, resulting a mixture of organic products with two major components, the expected dimer **4** and the known benzylated diiminopyridine derivative 4-Bn-ⁱPrBIP, identified by comparison of the ¹H-NMR signals with the spectra of these materials.¹² The relative signal intensities indicate that these products were formed in *ca.*1:2 ratio, indicating that only one half of the starting **2b** had undergone dimerization. The remaining was transformed into an NMR-silent species, revealed only after the mixture was subjected to demetallation. We concluded that, as shown in Scheme 4, this compound is probably the paramagnetic compound [AlEt₂(4-Bn-ⁱPrBIP)], similar to other paramagnetic aluminium compounds containing a singly-reduced (4-Bn-ⁱPrBIP)⁻ radical anion ligand bound to the Al(III)Et₂ fragment. As mentioned before, similar Al species with non-innocent BIP ligands, [AlR₂(ⁱPrBIP)] have been described in the literature, which bearing organic radical character, are virtually undetectable with conventional NMR spectroscopy. The formation of such product involves aromatization of the dihydropyridine by loss of the hydrogen atom from the benzylated position 4, a process analogous to the spontaneous dehydrogenation that we previously observed in the related organomanganese chemistry.



Scheme 5.

In addition, scheme 5 also depicts the thermal transformations undergone by complexes **2'b** and **2'c**. In these cases, heating the samples at 110 °C led to the complete disappearance of

any NMR resonances other than the residual peak of the solvent or background impurity traces. The demetallation protocol afforded organic mixtures whose spectra showed no sign of the tricyclic base **4'**, but mixtures of alkylated (4-allyl-ⁱPrBIP) and non-alkylated ⁱPrBIP, in grossly 1:1 ratio, slightly biased to the ally products in the case of **2'c**. The implication of this finding is that, for **2'b** or **2'c**, spontaneous de-alkylation becomes competitive with dehydrogenation, probably because the elimination of a stabilized allyl radical is a favourable process. In this case, aromatization of the dihydropyridine ring appears to become relatively fast and outcompetes the dimerization reaction.

The clean dimerization reactions experienced by complexes **2a** and **2'a** provides the hitherto only known examples of this process that do proceed from well-defined, isolated, and diamagnetic starting materials, hence amenable of detailed study by NMR. Therefore, we decided to study the relatively fast dimerization of **2'a** in order to obtain the kinetic parameters of such transformation. Hence, we monitored the evolution of NMR samples in toluene-*d*₈ of known concentration at five different temperatures evenly distributed over a 50 K interval (323 -373 K). Each sample was independently prepared and the evolution of selected ¹H resonances of both the reagent and product was monitored over the time. Figure 5 shows individual second order kinetic plots (top) and the Eyring graphic of the corresponding reaction rates (below). As can be seen, the experimental data show good linear fits,¹⁸ consistent with second order kinetics. The strongly negative activation entropy ($\Delta S^\ddagger = -53 \text{ cal}\cdot\text{mol}^{-1}\cdot\text{K}^{-1}$) is consistent with the expected restriction of freedom degrees as two reactant particles approach in the adequate orientations to reach the transition state. These features support Budzelaar's bimolecular mechanism and rule out that the reaction rate could be controlled by the pre-activation of one of the monomeric molecules, e. g., by thermal promotion to an excited diradical state, or interacting with some reactive intermediate present in a low stationary concentration, as we proposed for the O₂-triggered dimerization of Mn(II) dihydropyridinate species, since such mechanisms would exhibit unimolecular kinetics. Although the free energy barrier estimated by Budzelaar's DFT calculation, 13.4 Kcal·mol⁻¹ at 273 K, is considerably lower than the free activation energy extrapolated from the experimental data for the same conditions (26.3 Kcal·mol⁻¹), the difference can be attributed to the effect of steric hindrance in the real system, much smaller in the simplified molecular model. In fact, the experimental activation enthalpy ($\Delta H^\ddagger = 11.8 \text{ Kcal/mol}$) is very close to the computational electronic (SCF) energy barrier (12.1 Kcal·mol⁻¹). Thus, our kinetic data can be regarded in full agreement with the bimolecular mechanism proposed for the computational model.

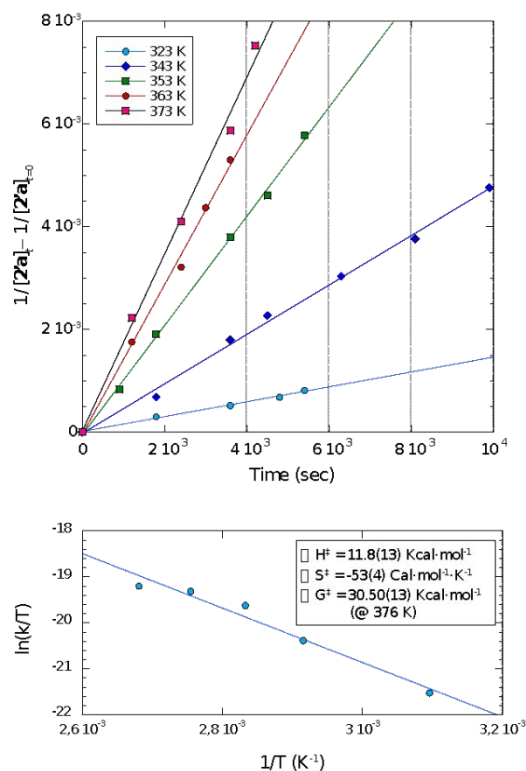


Figure 5. Second order kinetic plots for the dimerization of **2'a** at different temperatures (up) and Eyring plot of the reaction rates, showing the activation parameters deduced from the data fit (ΔG^\ddagger has been interpolated at 376 K, the average of the five temperatures used in the study).

Conclusions

Previously developed reactions of $i\text{PrBIP}$ and manganese(II) or zinc(II) alkyls followed by controlled demetallation provide selective access to 2,6-diimino-4-alkyl-1,4-dihydropyridines (4-R- $i\text{PrH}_2\text{BIP}$, R = benzyl or allyl). These ligands can be coordinated to aluminium alkyls AlR'_3 neutralizing their weakly acidic NH bonds with concomitant elimination of the corresponding alkane. This represents the first selective route to aluminium dihydropyridinates $[\text{AlR}'_2(4\text{-R-}i\text{PrBIPH})]$. The reactions with trimethylaluminium or triethylaluminium are facile and quantitative, whilst those involving bulkier triisobutylaluminium requires more forcing conditions. Although all these dihydropyridinates are thermally stable ($< 50 \text{ }^\circ\text{C}$) in the solid state or in solution, at higher temperatures, they change to yield either binuclear complexes that arise from ring fusion at carbons 3,5 of the dihydropyridine ring, or mononuclear aluminium species as result of spontaneous aromatization of the dihydropyridine with either H \cdot or R \cdot release. The efficiency of the dimerization reaction is very sensitive to steric effects, being the only process detected for $\text{R}' = \text{Me}$ but becoming unfavourable for $\text{R}' = \text{Et}$ or $i\text{Bu}$. Kinetics confirms such dimerization as a spontaneous bimolecular process with a strongly negative activation entropy, compatible with a previous mechanistic proposal based on DFT calculations. These results pave the way to the investigation of 4-R- H_2BIP and their dimers $(4\text{-R-}\text{H}_2\text{BIP})_2$ as new types of N_3 pincer ligands with many potential applications in Coordination and Organometallic Chemistry, Catalysis or the design of new materials.

Experimental

Most of the compounds included in this contribution are sensitive to traces of oxygen and water. Therefore, all manipulations were carried out under inert atmosphere Schlenk techniques or/and a N₂-filled glove box. The solvents employed (toluene, hexane, dichlorometane, pentane and tetrahydrofurane) were rigorously dried, distilled and degassed prior use. Anhydrous methanol was obtained after refluxed over carefully dried sodium methoxide, distilled and stored in a glass ampoule over activated molecular sieves. NMR spectra were recorded on Bruker Avance III-400 and DRX-400 spectrometers (FT 400 MHz, ¹H; 100 and 125 MHz, ¹³C). The ¹H and ¹³C{¹H} resonances of the solvent were used as the internal standard but the chemical shifts are reported with respect to tetramethylsilane (TMS). The assignments were regularly helped with 2D ¹H-¹H COSY, ¹H-¹³C HSQC and HMBC heterocorrelation NMR spectra. NMR-scale reactions (typically in a 0.02 mmol scale) were carried out in NMR tubes sealed with Teflon J. Young-type screw-cap valves. Benzene-d₆ and toluene-d₈ were dried over sodium benzophenone ketyl and vacuum distilled. Mass spectroscopy, elemental analysis and x-ray diffraction measurements were carried out in the Instituto de Investigaciones Químicas. AllylMgBr (1.0 M in Et₂O) was purchased from commercial vendors, being titrated prior used. Zinc dichloride (ZnCl₂) and the aluminium trialkyls (Me₃Al, Et₃Al 1.0 M in hexane and ⁱBu₃Al) were purchased from Sigma- Aldrich. Whilst zinc dichloride was purified by treatment with trimethylsilyl chloride, the aluminium compounds were used without purification or previous treatment. 2,6-[2,6-ⁱPr₂C₆H₃N=C(Me)₂C₅H₃N (ⁱPrBIP) was prepared by the condensation of 2,6-diacetylpyridine with 2,6-diisopropylaniline under azeotropic water-removal conditions and 2,6-[2,6-ⁱPr₂C₆H₃N=C(Me)₂-4-Bn-C₅H₄N (4-BnⁱPrH₂BIP (**1**)) was obtained according to our own methods, as described in the literature.¹⁴

Preparation of 4-Allyl-ⁱPrH₂BIP (1'**).** The method developed for the synthesis of **1**,¹⁴ did not produced satisfactory results when it was applied for the synthesis of 4-Allyl-ⁱPrH₂BIP (**1'**), since this allylic derivative was routinely obtained with variable amounts of the corresponding aromatized 4-Allyl-ⁱPrBIP.^{12,14} The preparation described below, entirely developed in the N₂-filled glovebox, represent an optimized procedure for the synthesis of **1'a** with respect of that reported by us in the literature.

A 30 mL scintillation vial was charged with 100 mg of ZnCl₂ (0.733 mmol) and 15 mL of THF in the N₂ filled glovebox. The resultant colourless solution was cooled at -60 °C. Then, 1.2 mL of a 1.18 M of AllylMgBr (1.750 mmol) in THF was added at -20 °C to the ZnCl₂ containing solution under vigorous stirring. A fine and greyish suspension was instantaneously formed, becoming a slightly grey solution after 5 minutes. The mixture was stirred for 30 minutes, cooled again to -20 °C and transferred to a suspension of ⁱPr⁴BIP (282 mg, 0.586 mmol) in 15 mL of THF, cooled at -60 °C. The resultant suspension was then stirred for 5 hours, period in which it turned from yellow to orange and finally to dark blue-greenish solution. Next, an excess of anhydrous MeOH (3mL) was added to the later

solution. The color of the mixture changed to dark red, evolving slowly to orange. Then, the solvents and volatiles were evaporated to dryness for 4 h, isolating a brown oily solid. This was extracted in hexane (2 x 20 mL) and upon filtration through a PTFE filter and evaporation to dryness, isolating 250 mg (82% yield) of corresponding to 4-Allyl-ⁱPrH₂BIP (**1'**) as dark orange foamy solid. Although the ¹H-NMR predominantly showed the resonances of the expected product, a set of tiny signals that could be attributed to other derivatives of ⁱPrBIP were also detected, but according to their relative integration, such species as a whole were in a proportion lower than 5% with in respect of the main product of the process. ¹H NMR (C₆D₆, 25 °C, 400 MHz), δ 1.10 (d, 12H, ³J_{HH} = 6.9 Hz, CHMeMe), 1.13 (d, 12H, ³J_{HH} = 6.9 Hz, CHMeMe), 1.69 (s, 6H, Me-C=N-), 2.29 (t, 2H, ³J_{HH} = 7.4 Hz, C₄Py-CH₂-CH=CH₂), 2.78 (hept, 4H, ³J_{HH} = 6.9 Hz, CHMeMe), 3.50 (m, 1H, 4-CH_{Py}), 5.03 (d, 2H, ³J_{HH} = 2.2 Hz, 3,5-CH_{Py}), 5.08-5.10 (overlapping multiplet, 2H, *cis, trans*-C₄Py-CH₂-CH=CH₂), 5.81 (m, 1H, C₄Py-CH₂CH=CH₂), 7.14 (m, 6H, CH_{N-Ar}), 8.89 (s, 1H, NH_{Py}).

Synthesis of [Al(Me)₂(4-Bn-ⁱPrHBIP)] (2a**).** A cold (-30 °C) colourless toluene solution (15 mL) of Me₃Al (45.9 μL, 0.48 mmol) was added slowly over another toluene yellow solution (15 mL) of **1** (250 mg, 0.43 mmol) at the same temperature and vigorously stirred in a 60 mL scintillation glass vial. The resultant mixture instantaneously changes from yellow to dark purple. This was allowed to gradually reach the room temperature and after 1 h stirring, it was evaporated to dryness, leaving a purple oily solid residue. Its ¹H-NMR spectrum showed the signals complex **2a**. Then, the solid was dissolved in 25 mL of hexane and filtered. The resulting solution was evaporated under reduced pressure to dryness (4 h), yielding 269 mg of a purple microcrystalline solid. Yield: 97%. Next, 100 mg of **2a** were dissolved in hexane (10 mL), filtered and partially evaporated. The concentrated purple solution was stored at -20 °C. After 24 h, dark pink plates crystals corresponding to compound **2a** had crashed, although they were not suitable enough for their X-ray diffraction resolution. ¹H NMR (C₇D₈, 25 °C, 400 MHz), δ -0.71 (s, 3H, CH₃Al), -0.70 (s, 3H, CH₃Al), 0.93 (d, ³J_{HH} = 6.7 Hz, 6H, CHMeMe), 0.99 (d, ³J_{HH} = 6.7 Hz, 6H, CHMeMe), 1.35 (dd, ³J_{HH} = 6.8, 1.9 Hz, 12H, CHMeMe), 1.72 (s, 6H, Me-C=N-), 2.80 (d, ³J_{HH} = 6.9 Hz, 2H, CH_{2, Py-Bn}), 2.94 (m, ³J_{HH} = 6.7 Hz, 4H, CHMeMe), 4.00 (m, 1H, 4-CH_{Py}), 5.07 (d, ³J_{HH} = 3.9 Hz, 2H, 3,5-CH_{Py}), 7.11 (m, 6H, CH_{N-Ar}), 7.22 (m, 5H, CH_{Ar, Py-Bn}). ¹³C{¹H} NMR (C₆D₆, 25 °C, 100 MHz), δ -7.0 (MeAl), -6.8 (MeAl), 17.2 (Me-C=N), 24.4 (CHMeMe), 25.6 (CHMeMe), 28.4 (CHMeMe), 39.6 (4-CH_{Py}), 47.9 (CH_{2, Py-Bn}), 106.7 (3,5-CH_{Py}), 124.5 (*p*-CH_{N-Ar}), 126.5 (*m*-CH_{N-Ar}), 126.9 (*p*-CH_{Ar, Py-Bn}), 128.8 (*o*-CH_{Ar, Py-Bn}), 129.9 (*m*-CH_{Ar, Py-Bn}), 139.4 (*i*-C_{Ar, Py-Bn}), 140.6 (2-C_{Py}), 142.2 (*o*-C_{N-Ar}), 142.5 (*i*-C_{N-Ar}), 171.0 (Me-C=N-). Anal. Calcd for C₄₂H₅₆AlN₃: C, 80.08; H, 8.96; N, 6.67. Found: C, 80.60; H, 8.40; N, 6.40.

Synthesis of [Al(Et)₂(4-Bn-ⁱPrHBIP)] (2b**).** The synthesis of **2b** was performed following the same experimental procedure than the above-described for the synthesis of **2a**. A 15 mL toluene solution containing 0.28 mL of a 1 M hexane solution of Et₃Al (0.280 mmol) was

mixed at -30 °C with another 15 mL toluene solution (150 mg, 0.261 mmol) of 4-Bn^{iPr}H₂BIP under stirring, which was kept during 2 h at room temperature. Upon isolating 157 mg of a dark purple microcrystalline solid (Yield: 91%), attempts for crystallization were carried out dissolving the product in 20 mL of hexane, filtering, concentrating the solution and storing it at -20 °C. After 24 h, a significant amount dark blue crystals that corresponded with **2b** unsuitable for X-ray diffraction studies were isolated. ¹H NMR (C₆D₆, 25 °C, 400 MHz), δ 0.21 (quart, ³J_{HH} = 8.0 Hz, 2H, Al-CH₂CH₃), 0.27 (quart, ³J_{HH} = 8.0 Hz, 2H, Al-CH₂CH₃), 0.99 (d, ³J_{HH} = 6.7 Hz, 6H, CHMeMe), 1.02 (overlapping triplet, 3H, Al-CH₂CH₃), 1.07 (d, ³J_{HH} = 6.7 Hz, 6H, CHMeMe), 1.15 (t, ³J_{HH} = 8.0 Hz, 3H, Al-CH₂CH₃), 1.48 (dd, ³J_{HH} = 6.8, 1.9 Hz, 12H, CHMeMe), 1.74 (s, 6H, Me-C=N-), 2.99 (d, ³J_{HH} = 7.1 Hz, 2H, CH₂, Py-Bn), 3.08 (m, 4H, CHMeMe), 4.11 (m, 1H, 4-CH_{Py}), 5.15 (d, ³J_{HH} = 4.0 Hz, 2H, 3,5-CH_{Py}), 7.22 (m, 6H, CH_{N-Ar}), 7.26 (m, 5H, CH_{Ar}, Py-Bn). ¹³C{¹H} NMR (C₆D₆, 25 °C, 100 MHz), δ 0.9 (Al-CH₂CH₃), 10.3 (Al-CH₂CH₃), 16.9 (Me-C=N-), 24.2 (CHMeMe), 25.4 (CHMeMe), 28.3 (CHMeMe), 39.6 (4-CH_{Py}), 48.2 (CH₂, Py-Bn), 106.4 (3,5-CH_{Py}), 124.4 (*p*-CH_{N-Ar}), 126.5 (*m*-CH_{N-Ar}), 126.8 (*p*-CH_{Ar}, Py-Bn), 128.8 (*o*-CH_{Ar}, Py-Bn), 129.9 (*m*-CH_{Ar}, Py-Bn), 139.3 (*i*-C_{Ar}, Py-Bn), 140.5 (2-C_{Py}), 142.6 (*o*-C_{N-Ar}), 143.1 (*i*-C_{N-Ar}), 171.8 (Me-C=N-). Anal. Calcd for C₄₄H₆₀AlN₃: C, 80.32; H, 9.19; N, 6.39. Found: C, 80.63; H, 9.14; N, 6.01.

Synthesis of [Al(Buⁱ)₂(4-Bn-^{iPr}HBIP)] (2c). This synthesis was carried out at NMR-tube scale. A 0.4 mL C₇D₈ yellow solution of **1** (15.4 mg; 0.026 mmol) was prepared in a 5 mL scintillation vial which was cool down to -25 °C. Another 0.3 mL C₇D₈ colorless solution of ⁱBu₃Al (6.7 μL; 0.026 mmol) was prepared and stored at the same temperature for 20 min. Then, the organoaluminium solution was slowly added via pipette at the above-mentioned temperature and the colour of the resultant mixture changed dramatically to dark blue. Then, the reaction mixture solution was transferred to NMR tube sealed with Teflon J. Young-type tap and a ¹H-NMR was recorded after 5 min at room temperature. After 2h at 23°C, the ¹H-NMR did not show significant changes rather than the signals of the corresponding compound **2c**, but in a relative ratio of less than 5% with respect of the signals of its precursors (**1** and ⁱBu₃Al). The blue toluene solution was heated at 60 °C. After 14 h, its color had changed to burgundy and the ¹H-NMR showed the signals of **2c** and those of both starting materials in a relative ratio of ca. 3:1 (**1**, for both **1** and ⁱBu₃Al). The reaction was completed after 72 h at 60 °C. ¹H NMR (C₇D₈, 25 °C, 400 MHz), δ 0.01 (bs, 2H, Al-CH₂CHMe₂), 0.13 (bs, 2H, Al-CH₂CHMe₂), 0.84 (bs, 6H, Al-CH₂CHMe₂), 0.89, 0.97, 1.05 (d, ³J_{HH} = 6.5 Hz, 18H, Al-CH₂CHMe₂, CHMeMe, CHMeMe), 1.44 (d, ³J_{HH} = 4.1 Hz, 12H, CHMeMe), 1.63 (m, 2H, Al-CH₂CHMe₂), 1.70 (s, 6H, Me-C=N-), 2.93 (d, ³J_{HH} = 7.3 Hz, 2H, CH₂, Py-Bn), 3.09 (bs, 4H, CHMeMe), 4.01 (m, ³J_{HH} = 3.4 Hz, 1H, 4-CH_{Py}), 5.08 (d, ³J_{HH} = 4.0 Hz, 2H, 3,5-CH_{Py}), 7.01-7.05 (bs, 6H, CH_{N-Ar}), 7.19 (bs, 5H, CH_{Ar}, Py-Bn). ¹³C{¹H} NMR (C₇D₈, 25 °C, 100 MHz), δ 16.6 (Me-C=N-), 21.6 (Al-CH₂CHMe₂), 23.8 (Al-CH₂CHMe₂), 23.9 (Al-CH₂CHMe₂), 25.0 (CHMe₂), 27.8 (Al-CH₂CHMe₂), 28.0 (Al-CH₂CHMe₂), 39.3 (4-CH_{Py}), 47.9 (CH₂, Py-Bn), 106.0 (3,5-CH_{Py}), 123.9 (*p*-CH_{N-Ar}), 126.0 (*m*-CH_{N-Ar}), 126.2 (*p*-CH_{Ar}, Py-Bn), 129.3

(*m*-CH_{Ar, Py-Bn}), 138.8 (*i*-C_{Ar, Py-Bn}) 139.9 (2-C_{Py}), 142.1 (*o*-C_{N-Ar}), 142.6 (*i*-C_{N-Ar}), 171.5 (Me-C=N-).

Synthesis of [Al(Me)₂(4-Allyl-ⁱPrHBIP)] (2[′]a). The same experimental conditions and procedure above-described for the synthesis of compounds **2a-c** was used for the synthesis of **2[′]a**. 20.1 μL (0.210 mmol) of Me₃Al were dissolved in 15 mL of toluene, which was cold at -30 °C and added to another 15 mL toluene solution of 4-AllylⁱPrBIPH₂ (**1[′]**, 100 mg, 0.191 mmol) at -30 °C. A dark blue microcrystalline solid was obtained in hexane at -20 °C, which upon filtration and drying, yielded 97 mg (82 %). Proper single crystals for X-ray diffraction studies appeared from a concentrated hexane solution stored at -20 °C after 24 h. ¹H NMR (C₆D₆, 25 °C, 400 MHz), δ -0.70 (s, 3H, CH₃Al), -0.69 (s, 3H, CH₃Al), 0.93 (t, ³J_{HH} = 4.6 Hz, 12H, CHMeMe), 1.33 (dd, ³J_{HH} = 11.9, 6.6 Hz, 12H, CHMeMe), 1.75 (s, 6H, Me-C=N-), 2.29 (t, ³J_{HH} = 6.7 Hz, 2H, C_{4Py}-CH₂-CH=CH₂), 2.93 (m, 4H, CHMeMe), 3.74 (m, 1H, 4-CH_{Py}), 5.09 (overlapping multiplet, 4H, *cis, trans*-C_{4Py}-CH₂-CH=CH₂) and 3,5-CH_{Py}), 5.83 (m, 1H, C_{4Py}-CH₂-CH=CH₂), 7.09 (m, 6H, CH_{N-Ar}). ¹³C{¹H} NMR (C₇D₈, 25 °C, 100 MHz), δ -7.2 (MeAl), -6.9 (MeAl), 17.0 (Me-C=N-), 24.2 (CHMeMe), 25.4 (CHMeMe), 28.3 (CHMeMe), 37.2 (4-CH_{Py}), 45.9 (C_{4Py}-CH₂-CH=CH₂), 106.5 (3,5-CH_{Py}), 116.6 (C_{4Py}-CH₂-CH=CH₂), 124.2 (*p*-CH_{N-Ar}), 126.7 (*m*-CH_{N-Ar}), 136.1 (C_{4Py}-CH₂-CH=CH₂), 140.5 (2-C_{Py}), 142.1 (*o*-C_{N-Ar}), 142.3 (*i*-C_{N-Ar}), 170.8 (Me-C=N-). Anal. Calcd for C₃₈H₅₄AlN₃: C, 78.71; H, 9.39; N, 7.25. Found: C, 78.47; H, 9.60; N, 7.30.

Synthesis of [Al(Et)₂(4-Allyl-ⁱPrHBIP)] (2[′]b). The experimental procedure described above for the synthesis of the analog systems **2b** was developed for the synthesis of complex **2[′]b**. 0.20 mL of a 1 M hexane solution of Et₃Al (0.200 mmol) were diluted in 15 mL of toluene and added to another 15 mL toluene solution of **1[′]** (100 mg, 0.191 mmol). A dark pink solid (110 mg, 95 %) corresponding with compound **2[′]b** were isolated after solvent and volatiles removal at reduce pressure. Recrystallization from a hexane concentrated solution produced a microcrystalline solid after 24 h at -20 °C. ¹H NMR (C₇D₈, 25 °C, 400 MHz), δ 0.05 (quart, ³J_{HH} = 8.0 Hz, 2H, Al-CH₂CH₃), 0.14 (quart, ³J_{HH} = 8.0 Hz, 2H, Al-CH₂CH₃), 0.84 (t, ³J_{HH} = 8.0 Hz, 3H, Al-CH₂CH₃), 0.98 (dd, ³J_{HH} = 8.7, 6.9 Hz, 12H, CHMeMe), 1.02 (overlapping triplet, 3H, Al-CH₂CH₃), 1.40 (t, ³J_{HH} = 6.4 Hz, 12H, CHMeMe), 1.77 (s, 6H, Me-C=N-), 2.34 (t, ³J_{HH} = 6.9 Hz, 2H, C_{4Py}-CH₂-CH=CH₂), 3.00 (m, 4H, CHMeMe), 3.75 (m, 1H, 4-CH_{Py}), 5.09 (d, ³J_{HH} = 4.0 Hz, 2H, 3,5-CH_{Py}), 5.14 (overlapping multiplet, 2H, *cis, trans*-C_{4Py}-CH₂-CH=CH₂), 5.90 (m, 1H, C_{4Py}-CH₂-CH=CH₂), 7.04 (m, 6H, CH_{N-Ar}). ¹³C{¹H} NMR (C₇D₈, 25 °C, 100 MHz), δ 10.2 (Al-CH₂CH₃), 16.8 (Me-C=N-), 23.9 (CHMeMe), 24.1 (CHMeMe), 25.2 (Al-CH₂CH₃), 28.2 (CHMeMe), 37.1 (4-CH_{Py}), 46.0 (C_{4Py}-CH₂-CH=CH₂), 106.2 (3,5-CH_{Py}), 116.5 (C_{4Py}-CH₂-CH=CH₂), 124.2 (*p*-CH_{N-Ar}), 126.7 (*m*-CH_{N-Ar}), 136.1 (C_{4Py}-CH₂-CH=CH₂), 140.3 (2-C_{Py}), 142.6 (*o*-C_{N-Ar}), 143.0 (*i*-C_{N-Ar}), 171.5 (Me-C=N-). Anal. Calcd for C₄₀H₅₈AlN₃: C, 79.03; H, 9.62; N, 6.91. Found: C, 79.84; H, 9.79; N, 6.80.

Synthesis of [Al(Buⁱ)₂(4-Allyl-ⁱPrHBIP)] (2^c). The same experimental procedure used for the synthesis of the previous 5 complexes was also applied for the synthesis of 2^c, although in this case, the reaction completion required for the aid of heat (60 °C) during several hours. A cold (-30 °C) colorless 20 mL toluene solution of 50 μL (0.198 mmol) of ⁱBu₃Al was added to a yellow 20 mL toluene solution of 1^c (100 mg, 0.191 mmol) at the same temperature. The resultant solution changed instantaneously from yellow to dark violet. The mixture was then transferred into a 100 mL glass ampoule equipped with a Teflon J. Young-type screw-cap valve for sealing. The ampoule containing the reaction mixture was then heated at 60 °C inside of a silicone oil bath for 36 hours. Next, the solvents and volatiles were eliminated under vacuum, isolating a dark purple solid which was dissolved in hexanes, filtered and concentrated prior storing at -20 °C. Upon filtration and drying, a dark purple solid (112 mg, 88%) corresponding with compound 2^c was isolated. Several attempts for crystallization resulted fruitless. ¹H NMR (C₇D₈, 25 °C, 400 MHz), δ 0.03 (bs, 2H, Al-CH₂CHMe₂), 0.14 (bs, 2H, Al-CH₂CHMe₂), 0.89 (d, ³J_{HH} = 6.6 Hz, 6H, Al-CH₂CHMe₂), 1.01 (dd, ³J_{HH} = 12.6, 6.7 Hz, 12H, CHMeMe), 1.07 (d, ³J_{HH} = 6.5 Hz, 6H, Al-CH₂CHMe₂), 1.43 (t, ³J_{HH} = 6.6 Hz, 12H, CHMeMe), 1.62 (m, 1H, Al-CH₂CHMe₂), 1.75 (s, 6H, Me-C=N-), 1.97 (m, 1H, Al-CH₂CHMe₂), 2.39 (t, ³J_{HH} = 6.9 Hz, 2H, C₄Py-CH₂-CH=CH₂), 2.94 (bs, 2H, CHMeMe), 3.09 (bs, 2H, CHMeMe), 3.77 (m, ³J_{HH} = 6.9 Hz, 1H, 4-CH_{Py}), 5.09 (d, ³J_{HH} = 3.9 Hz, 2H, 3,5-CH_{Py}), 5.13 (overlapping multiplet, 2H, *cis, trans*-C₄Py-CH₂-CH=CH₂), 5.89 (m, 1H, C₄Py-CH₂-CH=CH₂), 7.04 (m, 6H, CH_{N-Ar}). ¹³C{¹H} NMR (C₆D₆, 25 °C, 100 MHz), δ 16.8 (Me-C=N-), 21.4 (Al-CH₂CHMe₂), 23.9 (Al-CH₂CHMe₂), 24.1 (Al-CH₂CHMe₂), 24.6 (CHMeMe), 25.1 (CHMeMe), 27.9 (Al-CH₂CHMe₂), 28.1 (Al-CH₂CHMe₂), 37.1 (4-CH_{Py}), 45.9 (C₄Py-CH₂-CH=CH₂), 106.3 (3,5-CH_{Py}), 116.4 (C₄Py-CH₂-CH=CH₂), 124.1 (*p*-CH_{N-Ar}), 126.4 (*m*-CH_{N-Ar}), 135.8 (C₄Py-CH₂-CH=CH₂), 140.0 (2-C_{Py}), 142.4 (*o*-C_{N-Ar}), 142.7 (*i*-C_{N-Ar}), 171.7 (Me-C=N-). Anal. Calcd for C₄₄H₆₆AlN₃: C, 79.59; H, 10.02; N, 6.33. Found: C, 79.28; H, 10.37; N, 6.10.

Dimerization of 2a. Synthesis of [Al(Me)₂(4-Bn-ⁱPrHBIP)]₂ (3a). A 30 mL toluene solution of compound 2a (200 mg, 0.318 mmol) was prepared in a 100 mL Schlenck inside the N₂-filled glovebox. Then, this was taken out, interfaced to a vacuum/argon line and placed into a silicone oil bath heated up to 110 °C. The solution was then stirred at such temperature for a period of 36 h. Next, solvents and volatiles were removed at dryness, isolating 184 mg (yield 92%) of a dark purple solid that corresponds with the dimer 3a. Its crystallization was performed by taking a sample of 100 mg of such a powdery solid and dissolved it in 10 mL of hexane. Then, such solution was concentrated to its half and 0.1 mL of dichloromethane was added to it, prior storing at -25 °C. After 48 h, dark pink plate crystals which were suitable for X-ray diffraction studies were obtained. ¹H NMR (C₇D₈, 25 °C, 400 MHz): δ -0.57 (s, 6H, CH₃Al), -0.49 (s, 6H, CH₃Al), 1.10 (d, ³J_{HH} = 6.8 Hz, 12H, CHMeMe), 1.19 (d, ³J_{HH} = 6.8 Hz, 12H, CHMeMe), 1.35 (d, ³J_{HH} = 6.7 Hz, 12H, CHMeMe), 1.44 (d, ³J_{HH} = 6.7 Hz, 12H, CHMeMe), 1.76 (s, 12H, Me-C=N-), 2.25 (bs, ³J_{HH} = 4H, CH₂, Py-Bn), 2.88 (s, 4H, 3,5-CH_{Py}), 3.17 (m, 8H, CHMeMe), 7.02 (m, 12H, CH_{N-Ar}), 7.26 (m, 10H, CH_{Ar}, Py-Bn). ¹³C{¹H} NMR (C₇D₈,

25 °C, 100 MHz), δ 0.7 (*MeAl*), 1.7 (*MeAl*), 21.8 (*Me-C=N-*), 29.8 (*CHMeMe*), 30.0 (*CHMeMe*), 33.9 (*CHMeMe*), 37.0 (4-*CH_{Py}*), 44.4 (*CH₂*, *Py-Bn*), 48.6 (3,5-*CH_{Py}*), 129.0 (*p-CH_{N-Ar}*), 131.6 (*m-CH_{N-Ar}*), 131.8 (*p-CH_{Ar, Py-Bn}*), 134.6 (*o-CH_{Ar, Py-Bn}*), 135.1 (*m-CH_{Ar, Py-Bn}*), 145.6 (*i-C_{Ar, Py-Bn}*), 147.5 (2-*C_{Py}*), 147.8 (*o-C_{N-Ar}*), 148.6 (*i-C_{N-Ar}*), 169.6 (*Me-C=N-*). Anal. Calcd for $C_{84}H_{112}Al_2N_6$: C, 80.60; H, 8.96; N, 6.67. Found: C, 80.09; H, 9.01; N, 6.56.

Dimerization of 2a and demetallation. In a NMR tube sealed with Teflon J. Young-type tap, 20 mg (31.8 μ mol) of compound **2a** were dissolved in toluene- d_8 and heated up to 110 °C. Once dimerization was completed and the 1H -NMR showed just the signals of compound **3a** and no resonances of the starting material (**2a**) were left, an excess of dry methanol (2 mL) was added into the tube. The dark purple solution which changed quickly to orange was evaporated at vacuum to dryness, isolating a reddish orange oily solid. This crude was extracted with 2 x 5 mL of hexane, filtered through a pad of Celite and evaporated to dryness again. The resultant yellow oily-solid which was completely soluble in benzene- d_6 showed a 1H -NMR that included a single set of signals corresponding with those of the metal-free dimer (4-Bn- $iPrH_2BIP$) $_2$ as compared with that reported by us in the literature.¹⁸

Dimerization of 2'a. Synthesis of [Al(Me) $_2$ (4-Allyl- $iPrHBIP$)] $_2$ (3'a). The thermal treatment described above over **2a** was applied to **2'a**, using 95 mg (0.164 mmol) dissolved in 15 mL of toluene and stirring during 5 h at 110 °C. When solvent and volatiles were removed at reduced pressure, 80 mg (89 % Yield) of compound **3'a** were isolated. Suitable crystals for X-ray diffraction studies were obtained after dissolving 50 mg of **3'a** in hexane (10 mL), filtering, concentrating to half of the volume of such solution and storing it at -25 °C. 1H NMR (C_7D_8 , 25 °C, 400 MHz): δ -0.73 (s, 6H, *CH₃Al*), -0.46 (s, 6H, *CH₃Al*), 1.17 (dd, $^3J_{HH} = 6.8, 2.1$ Hz, 24H, *CHMeMe*), 1.34 (dd, $^3J_{HH} = 10.9, 6.8$ Hz, 24H, *CHMeMe*), 1.82 (m, 4H, *C_{4Py-CH₂-CH=CH₂}*), 1.87 (s, 12H, *Me-C=N-*), 2.02 (m, 2H, 4-*CH_{Py}*), 3.01 (s, 4H, 3,5-*CH_{Py}*), 3.12 (m, 4H, *CHMeMe*), 3.24 (m, 4H, *CHMeMe*), 5.09 (dd, $^3J_{HH} = 16.0, 11.6$ Hz, 4H, *C_{4Py-CH₂-CH=CH₂}*), 5.82 (m, 2H, *C_{4Py-CH₂-CH=CH₂}*), 7.02 (m, 12H, *CH_{N-Ar}*). $^{13}C\{^1H\}$ NMR (C_7D_8 , 25 °C, 100 MHz), δ -5.6 (*MeAl*), -2.5 (*MeAl*), 16.6 (*Me-C=N-*), 24.2 (*CHMeMe*), 24.3 (*CHMeMe*), 24.8 (4-*CH_{Py}*), 28.5 (*CHMeMe*), 29.1 (*CHMeMe*), 37.3 (*C_{4Py-CH₂-CH=CH₂}*), 43.6 (3,5-*CH_{Py}*), 116.6 (*C_{4Py-CH₂-CH=CH₂}*), 123.9 (*p-CH_{N-Ar}*), 126.4 (*m-CH_{N-Ar}*), 140.5 (*C_{4Py-CH₂-CH=CH₂}*), 142.2 (2-*C_{Py}*), 142.6 (*o-C_{N-Ar}*), 143.7 (*i-C_{N-Ar}*), 164.4 (*Me-C=N-*). Anal. Calcd for $C_{76}H_{108}Al_2N_6$: C, 78.71; H, 9.39; N, 7.25. Found: C, 78.72; H, 9.58; N, 7.28.

Dimerization of 2'a and demetallation. The same experimental procedure developed in the case of the thermal treatment of **2a** and subsequent demetallation was applied to **2'a**, obtaining similar results. At the end of process, a benzene- d_6 soluble orange-oily solid was obtained. Its 1H -NMR showed just a single set of signals, which corresponded with those of the organic ditopic dimer (4-Allyl- $iPrH_2BIP$) $_2$ as compared with the data reported in the literature.¹⁸

Monitoring the thermal treatment of 2b. Generation of [Al(Et)₂(4-Bn-ⁱPrHBIP)]₂ and [Al(Et)₂(4-Bn-ⁱPrBIP⁻¹)] and demetallation. Compound **2b** (20 mg, 30.4 μmol) was dissolved in toluene-*d*₈ before being transferred into an NMR tube sealed with Teflon J. Young-type tap inside the N₂-filled glovebox. The tube was then taken out from the glovebox and placed in a thermostatic bath at 110 °C. After 3h heating, the tube was removed from the heating bath, cooled down to room temperature and transferred to the NMR probe. The ¹H-NMR spectrum showed the signals of compound **2b** together with another set of resonances attributed to the dimer [Al(Et)₂(4-Bn-ⁱPrHBIP)]₂ (**3b**) ¹H NMR (C₆D₆, 25 °C, 400 MHz), δ 0.07 (quart, ³J_{HH} = 8.0 Hz, 4H, Al-CH₂CH₃), 0.37 (quart, ³J_{HH} = 8.0 Hz, 4H, Al-CH₂CH₃), 0.80 (t, ³J_{HH} = 8.1 Hz, 6H, Al-CH₂CH₃), 0.99 (t, 6H, Al-CH₂CH₃), 1.09 (m, 24H, CHMeMe), 1.40 (dd, 24H, CHMeMe), 1.58 (s, 12H, Me-C=N-), 3.12 (sept, ³J_{HH} = 6.6 Hz, 4H, CHMeMe), 3.24 (sept, ³J_{HH} = 6.7 Hz, 4H, CHMeMe) 7.12 (m, 12H, CH_{N-Ar}). Signals for 3,5-CH_{Py}, 4-CH_{Py} and PhCH₂ could not be assigned with confidence.

Once reaction was completed (16 h at 110 °C) based on the ¹H-NMR analysis, which only showed the signals of compound **3b** and no resonances of the starting material (**2b**) were left, an excess of dry methanol (2 mL) was added into the tube. The dark purple solution changed quickly to orange, then it was evaporated at vacuum to dryness, resulting a reddish orange oily solid. This crude was extracted with 2 x 5 mL of hexane, filtered through a pad of Celite and evaporated to dryness again. The resultant yellow oily-solid, which was completely soluble in benzene-*d*₆, showed a ¹H-NMR that included two sets of signals corresponding with those of the metal-free dimer (4-Bn-ⁱPrH₂BIP)₂ together with the ones of 4-Bn-ⁱPrBIP as compared with the spectra of such compounds reported by us in the literature.¹⁸ The ¹H-NMR showed both species in an approximately relative ratio of 1:2.

Monitoring the thermal treatment of 2'b. Generation of [Al(Et)₂(4-Allyl-ⁱPrBIP⁻¹)] and [Al(Et)₂(ⁱPrBIP⁻¹)]

The same experimental procedure developed in the case of the thermal treatment of **2b** was applied to **2'b**. After 3 h heating at 110 °C, the ¹H-NMR signals of **2'b** had decreased but new resonances were not detected. The following ¹H-NMR spectra regularly recorded over a period of several hours in which the tube had been kept at 110 °C, showed only the signals of **2'b**, until they disappear after 30 h heating. This left a flat ¹H-NMR spectrum, excluding the peaks attributed to the deuterated solvent. The resultant solution was however dark purple. Then, an excess of dry methanol (2 mL) was added into the tube. The color of the solution changed to orange before being evaporated at vacuum to dryness. The resultant reddish orange oily solid was extracted with 2 x 5 mL of hexane, filtered through a pad of Celite and evaporated to dryness. The yellow oily-solid isolated which was completely soluble in benzene-*d*₆ showed a ¹H-NMR that included several sets of signals in which we could distinguish those of the known aromatic ligands ⁱPrBIP and 4-Allyl-ⁱPrBIP,¹² as the main products of the process.

Monitoring the thermal treatment 2'c. Generation of [Al(Buⁱ)₂(4-Allyl-ⁱPrBIP⁻¹)] and [Al(Buⁱ)₂(ⁱPrBIP⁻¹)]

The same experimental protocol carried out for the thermal treatment of 2'b followed by demetallation and isolation of the organic residue was applied to 2'c, obtaining comparable results. An orange-oily solid which was completely soluble in benzene-d₆ was obtained. Its ¹H-NMR included the signals of the known aromatic ligands ⁱPrBIP and 4-Allyl-ⁱPrBIP¹² as the main products heating of 2'c and subsequent demetallation.

Dimerization Kinetics of 2'a to 3'a.

The dimerization rate of compound 2'a was monitored by performing five NMR-tube scale experiments at five different temperatures distributed over a 50 K interval (323, 343, 353, 363 and 373 K). Samples containing 45 μmol of the complex in 0.6 ml of toluene-d₈ were prepared individually. We found operationally convenient to generate the complex directly in the NMR tube. In a nitrogen-filled glove-box, a 5 mL glass vial was charged with 23.7 mg (0.045 mmol) of 4-Allyl-HⁱPr⁴BIP 1'a and 0.4 mL of toluene-d₈, storing the yellow clear solution at -30 °C for 15 min. In another 5 mL vial, 0.2 mL toluene-d₈ solution of commercial Me₃Al (4.3 μL, 0.045 mmol) was prepared and also placed at -30 °C during 10 min. Then, both vials were brought out from the freezer and the aluminum alkyl was slowly transferred via pipette to the ligand (1'a) containing yellow solution resulting an instantaneous color change from yellow to dark burgundy. The reaction mixture was subsequently loaded into a J.-Young NMR tube, gently hand-shaked, and taken to the NMR probe, which had been stabilized at the prescribed temperature. The progress of the reaction was monitored every 15 min during 3 h by integration of selected signals of 2'a (2.92 ppm for the CH(ⁱPr) signals; 1.78 ppm for the Me-CN signal) and 3'a (centered at 3.24 ppm for the CH(ⁱPr) signals; 1.87 ppm for Me-CN the signal). The absolute concentration of 2'a in each measurement was calculated by assuming that its conversion into is quantitative, and the sum of intensities of analogous signals of 2'a and 3'a is constant and equal to the initial concentration of 2'a.

X-ray Structural Analysis for 2'a, 3a and 3'a: Crystals suitable for X-ray diffraction analysis were coated with dry perfluoropolyether, mounted on glass fibers, and fixed in a cold nitrogen stream to the goniometer head. Data collections were performed on a Bruker-Nonius X8 Apex-II CCD diffractometer, using graphite monochromatized Mo radiation ($\lambda(\text{Mo K}\alpha) = 0.71073 \text{ \AA}$) and fine-sliced ω and φ scans (scan widths 0.30° to 0.50°).¹⁹ The data were reduced (*SAINTE*) and corrected for absorption effects by the multiscan method (*SADABS*).²⁰ The structures were solved by direct methods (*SIR2002*, *SHELXS*) and refined against all F^2 data by full-matrix least-squares techniques (*SHELXL-2016/6*) minimizing $w[F_o^2 - F_c^2]^2$.²¹ All non-hydrogen atoms were refined with anisotropic displacement parameters. Hydrogen atoms were included in calculated positions and allowed to ride on their carrier atoms with the isotropic temperature factors U_{iso} fixed at 1.2 times (1.5 times for methyl groups) of the U_{eq} values of the respective carrier atoms. In the crystal structure of 2'a the central ring

bearing the allyl group appears disordered on both sides of the coordination plane forming the pincer ligand with the metal, so this group was modeled in two sets of sites. At the end of the refinement, occupancy ratio was set at 0.55:0.45. Moreover, a search for solvent accessible voids in **2'a** using *PLATON*,²² showed some small volumes of potential solvents less than 40 Å³, impossible to model even with the most severe restraints. The corresponding CIF data represent *SQUEEZE*²³ treated structures with the solvent molecules handling as a diffuse contribution to the overall scattering, without specific atom position and excluded from the structural model. The *SQUEEZE* results were appended to the CIF. The crystal structure of **3a** appears with the benzyl group slightly disordered and was modeled in two sets of sites and the occupancy ratio was set at 0.53:0.47. Together with this crystal structure a dichloromethane molecule is also observed as a crystallization solvent. The crystal structure of **3'a** was refined as a two-component TWIN with 0.533:0.467 domain ratio. Next to this crystal structure a n-hexane molecule is also observed as a crystallization solvent. The modeling of the observed disorders described above required some geometric restraints (DFIX instruction), the ADP restraint SIMU and the rigid bond restraint DELU were used in order to obtain more reasonable geometric and ADP values of the disordered atoms. It was also useful to restraint the anisotropic U-values of these atoms to behave more isotropically (ISOR instruction).

Crystal data for 2'a: C₃₈H₅₄AlN₃, *M* = 579.82, *a* = 32.0061(10) Å, *b* = 32.0061(10) Å, *c* = 13.9450(5) Å, $\alpha = 90^\circ$, $\beta = 90^\circ$, $\gamma = 90^\circ$, *V* = 14285.1(10) Å³, *T* = 193(2) K, space group *I*4₁/*a*, *Z* = 16, $\mu = 0.085 \text{ mm}^{-1}$, 80463 reflections measured, 6454 independent reflections (*R*_{int} = 0.0941). The final *R*₁ values were 0.0480 (*I* > 2σ(*I*)). The final *wR*(*F*²) values were 0.1228 (*I* > 2σ(*I*)). The final *R*₁ values were 0.0939 (all data). The final *wR*(*F*²) values were 0.1384 (all data). The goodness of fit on *F*² was 0.975.

Crystal data for 3a: C₈₄H₁₁₂Al₂N₆•2(CH₂Cl₂), *M* = 1429.60, *a* = 13.2320(4) Å, *b* = 16.7149(5) Å, *c* = 19.4032(6) Å, $\alpha = 90^\circ$, $\beta = 102.4510(10)^\circ$, $\gamma = 90^\circ$, *V* = 4190.5(2) Å³, *T* = 193(2) K, space group *P*2₁/*n*, *Z* = 2, $\mu = 0.208 \text{ mm}^{-1}$, 30216 reflections measured, 7583 independent reflections (*R*_{int} = 0.0214). The final *R*₁ values were 0.0431 (*I* > 2σ(*I*)). The final *wR*(*F*²) values were 0.1147 (*I* > 2σ(*I*)). The final *R*₁ values were 0.0527 (all data). The final *wR*(*F*²) values were 0.1204 (all data). The goodness of fit on *F*² was 1.084.

Crystal data for 3'a: C₇₆H₁₀₈Al₂N₆•C₆H₁₄, *M* = 1245.81, *a* = 10.5741(14) Å, *b* = 12.4548(16) Å, *c* = 16.270(2) Å, $\alpha = 74.182(3)^\circ$, $\beta = 76.401(3)^\circ$, $\gamma = 75.500(4)^\circ$, *V* = 1963.7(5) Å³, *T* = 193(2) K, space group *P* $\bar{1}$, *Z* = 1, $\mu = 0.081 \text{ mm}^{-1}$, 5872 reflections measured, 5872 independent reflections. The final *R*₁ values were 0.0690 (*I* > 2σ(*I*)). The final *wR*(*F*²) values were 0.1571 (*I* > 2σ(*I*)). The final *R*₁ values were 0.1224 (all data). The final *wR*(*F*²) values were 0.1784 (all data). The goodness of fit on *F*² was 1.062.

Author Information

^a Manuel Gallardo-Villagrán, Dr. Eleuterio Álvarez, Dra. Pilar Palma, Dr. Juan Cámpora, and Dr. Antonio Rodríguez-Delgado Instituto de Investigaciones Químicas, CSIC-Universidad de Sevilla. c/ Américo Vespucio, 49, 41092, Sevilla, Spain. E-mail: antonior@iiq.csic.es

^b Dr. Fernando Vidal, Department of Chemistry, Rutgers University, Newark, 73, Warrent St. Newark NJ 07102

^c Dr. Eugene Y.-X. Chen, Department of Chemistry, Colorado State University, Fort Collins, Colorado 80523-1972.

Electronic supplementary information (ESI) available.

CCDC 1898737 for **2'a**, 1898738 for **3a** and 1898739 for **3'a**

Acknowledgement

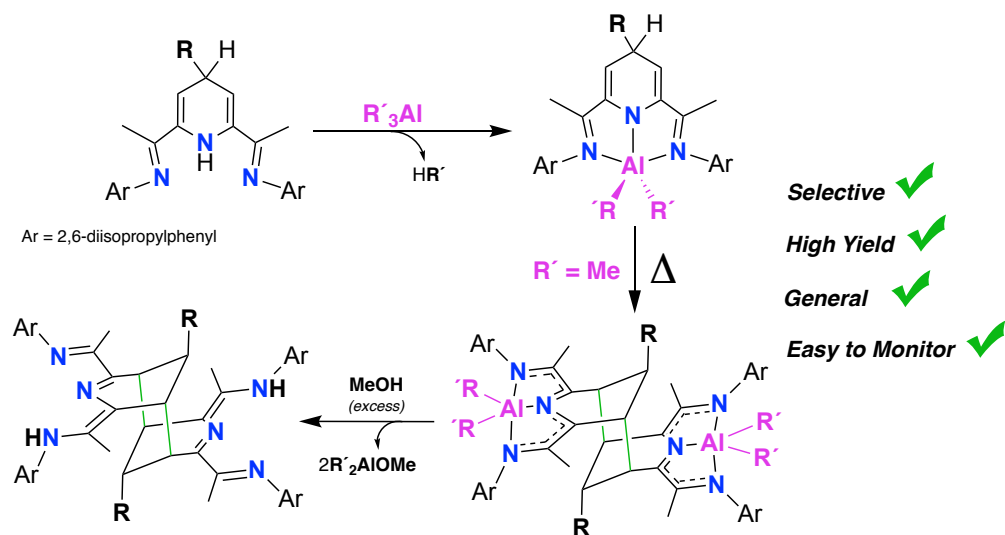
The Spanish Ministry of Economy and Innovation (MINECO) and the FEDER funds of the European Union supported this work through the grants CTQ2015-68978-P and PRX14/00339, last one included in the program "Salvador Madariaga". The work done at CSU was supported by the United States National Science Foundation (CHE-1664915).

References

- 1) a) Q. Knijnenburg, S. Gambarotta, P.H.M. Budzelaar, Dalton Trans. (2006) 5442-5448. b) V.C. Gibson, C. Redshaw, G.A. Solan, Chem. Rev. 107 (2007) 1745-1776. c) J. Cámpora, A. Rodríguez-Delgado, Pilar Palma. *PINCER COMPOUNDS, 1st Ed, Chemistry and Applications*, Eds. D. Morales-Morales (2018), 26, 539-582.
- 2) a) M. Bruce, V. C. Gibson, C. Redshaw, G. A. Solan, A. J. P. White, D. J. Williams, Chem. Commun. (1998) 2523-2524. b) G. J. P. Britovsek, V. C. Gibson, S. Mastroianni, D. C. H. Oakes, C. Redshaw, G. A. Solan, A. J. P. White, D. J. Williams. J. Eur. J. Inorg. Chem. 2001, 431-437.
- 3) S. Milione, G. Cavallo, C. Tedesco, A. Grassi, J. Chem. Soc., Dalton Trans. (2002) 1839-1846.
- 4) a) Q. Knijnenburg, J.M.M. Smits, P.H.M. Budzelaar, Organometallics 25 (2006) 1036-1046. b) Q. Knijnenburg, J.M.M. Smits, P.H.M. Budzelaar, C. R. Chimie 2004 (2004) 865-869.
- 5) B. Y. Tay, C. Wang, S. C. Chia, L. P. Stubbs, P. K. Wong, M. van Meurs, Organometallics 30, (2011) 6028-6033.
- 6) a) B. L. Small, M. Brookhart, A. M. A. Bennett, J. Am. Chem. Soc. 120 (1998) 4049-4050. b) G. J. P. Britovsek, V. C. Gibson, S. J. McTavish, G. A. Solan, A. J. P. White, D. J. Williams, B. S. Kimberley, P. J. Maddox, (1998) 849-850.

- 7) O.R. Luca, R. H. Crabtree, *Chem. Soc. Rev.*, 42 (2013) 1440 – 1459. (b) S. Blanchard, D. Derat, M. Desage-El Murr, L. Fensterbank, M. Malacria, V. Mouriès-Mansuy, *Eur. J. Inorg. Chem.*, (2012) 376-389.
- 8) a) L. A. Berben, *Chem. Eur. J.* 21 (2015) 2724 - 2742. b) T. W. Myers, T. J. Sherbow, J. C. Fettinger, L. A. Berben, *Dalton Trans.*, 45 (2016) 5989 – 5998.
- 9) H. Sugiyama, G. Aharonian, S. Gambarotta, G.P.A. Yap, P.H.M. Budzelaar, *J. Am. Chem. Soc.*, 124 (2002) 12268-12274.
- 10) J. Scott, S. Gambarotta, I. Korobkov, Q. Knijnenburg, B. de Bruin, P. H. M. Budzelaar, *J. Am. Chem. Soc.*, 127 (2005) 17204-17206
- 11) M. A. Cartes, A. Rodríguez-Delgado, P. Palma, E. Álvarez, J. Cámpora, *Organometallics* 33 (2014) 1834-1839.
- 12) a) J. Cámpora, C. M. Pérez, A. Rodríguez-Delgado, A. M. Naz, P. Palma, E. Álvarez, *Organometallics* 26 (2007) 1104-1107. b) C. M. Pérez, A. Rodríguez-Delgado, P. Palma, E. Álvarez, E. Gutiérrez-Puebla, J. Cámpora, *Chem. Eur. J.*, 16 (2010) 13834-13842.
- 13) I. Fernández, R. J. Trovich, E. Lobkovsky, P. J. Chirik, *Organometallics* 27 (2008) 109-118.
- 14) J. Sandoval, P. Palma, E. Álvarez, A. Rodríguez-Delgado, J. Cámpora, *Chem. Commun.* 49 (2013) 6791 – 6793.
- 15) J. J. Sandoval, P. Palma, E. Álvarez, J. Cámpora, A. Rodríguez-Delgado, *Organometallics* 35 (2016) 3197-3204.
- 16) M. Arrowsmith, M. S. Hill, G. Kociok-Köhn, *Organometallics* 29 (2010) 4203-4206.
- 17) J. J. Sandoval, C. Melero, P. Palma, E. Álvarez, A. Rodríguez-Delgado, J. Cámpora, *Organometallics* 35 (2016) 3336 – 3343
- 18) The data dispersion in the Eyring plot can be safely attributed to experimental error in the rate constants, originating in the concentration uncertainty, and are not significant from the statistical or mechanistic points of view. We have checked that slight corrections of the experimental concentrations can be fitted to produce a perfect linear correlation with little change in the final values of the activation parameters, but we refrained to use other than the original datapoints.
- 19) Bruker *APEX2*; Bruker AXS, Inc.; Madison, WI, 2007.
- 20) Bruker Advanced X-ray solutions. *SAINT* and *SADABS* programs. Bruker AXS Inc. Madison, WI, 2004.
- 21) M. C. Burla, M. Camalli, B. Carrozzini, G. L. Casciarano, C. Giacovazzo, G. Polidori and R. Spagna, SIR2002: the Program. *J. Appl. Crystallogr.* (2003), 36, 1103 – 1104.
- 22) A. L. Spek, Single-crystal Structure Validation with the Program *PLATON*. *J. Appl. Crystallogr.*, (2003), 36, 7-13

23) P. v. d. Sluis and A. L. Spek, BYPASS: An Effective Method for the Refinement of Crystal Structures Containing Disordered Solvent Regions. *Acta Crystallogr., Sect. A.* (1990), *46*, 194-201.



2,6-bisimino-4-alkyl-1,4-dihydropyridines provides access to dihydropyridinate(-1) aluminium (III) dialkyls, their double cycloaddition dimerization products and the metal-free ditopic ligands after controlled methanolysis.